

Extraordinary optical transmission through multi-layered systems of corrugated metallic thin films

Choon How Gan^{1,2} and Greg Gbur¹

¹*Dept. of Physics and Optical Science, University of North Carolina at Charlotte, 9201 University City Boulevard, Charlotte, NC 28223, USA*

²*Current address: Laboratoire Charles Fabry de l'Institut d'Optique, CNRS, Univ Paris-Sud, Campus Polytechnique, 91127 Palaiseau cedex, France*

choon.gan@institutoptique.fr

Abstract: Optical transmission through multi-layered systems of corrugated metallic thin films is investigated by rigorous electromagnetic simulations based on an exact Green tensor method. Compared to a single metal slab of equivalent thickness and volume, it was found that the multi-layered system can significantly impede the field decay, often leading to transmission greater than that expected from the Fabry-Perot resonance-like behavior exhibited by subwavelength slits in a single slab. Extraordinary optical transmission is also observable for systems of layers whose combined thicknesses are much greater than the skin depth of the metal. Structures consisting of up to five layers with a net thickness of 500 nm for the metal films were considered in our study. These findings demonstrate that an appreciable fraction of the optical power that is incident on the thin metal films can be transmitted over distances greater than their skin depth using plasmonic resonances.

© 2009 Optical Society of America

OCIS codes: (240.6680) Surface plasmons; (310.4165) Multilayer design

References and links

1. T. W. Ebbesen, H. J. Lezec, H. F. Ghaemi, T. Thio, and P. A. Wolff, "Extraordinary optical transmission through sub-wavelength hole arrays," *Nature* **391**, 667-669 (1998).
2. H. F. Ghaemi, T. Thio, D. E. Grupp, T. W. Ebbesen, and H. J. Lezec, "Surface plasmons enhance optical transmission through subwavelength holes," *Phys. Rev. B* **58**, 6779-6782 (1998).
3. D. E. Grupp, H. J. Lezec, T. W. Ebbesen, K. M. Pellerin, and T. Thio, "Crucial role of metal surface in enhance transmission through subwavelength apertures," *Appl. Phys. Lett.* **77**, 1569-1571 (2000).
4. W. L. Barnes, W. A. Murray, J. Dintinger, E. Devaux, and T. W. Ebbesen, "Surface plasmon polaritons and their role in the enhanced transmission of light through periodic arrays of subwavelength holes in a metal film," *Phys. Rev. Lett.* **92**, 107401 (2004).
5. H. F. Schouten, N. Kuzmin, G. Dubois, T. D. Visser, G. Gbur, P. F. A. Alkemade, H. Blok, G. W. 't Hooft, D. Lenstra and E. R. Eliel, "Plasmon-assisted two-slit transmission: Young's experiment revisited," *Phys. Rev. Lett.* **94**, 053901 (2005).
6. P. Lalanne and J. P. Hugonin, "Interaction between optical nano-objects at metallo-dielectric interfaces," *Nature Phys.* **2**, 551-556 (2006).
7. H. Liu and P. Lalanne, "Microscopic theory of the extraordinary optical transmission," *Nature* **452**, 728-731 (2008).
8. Y. Ye and J. Zhang, "Enhanced light transmission through cascaded metal films perforated with periodic hole arrays," *Opt. Lett.* **30**, 1521-1523 (2005).
9. B. Bai, L. Li, and L. Zeng, "Experimental verification of enhanced transmission through two-dimensionally corrugated metallic films without holes," *Opt. Lett.* **30**, 2360-2362 (2005).

10. H. B. Chan, Z. Marcet, K. Woo, D. B. Tanner, D. W. Carr, J. E. Bower, R. A. Cirelli, E. Ferry E, F. Klemens, J. Miner, C. S. Pai, and J. A. Taylor, "Optical transmission through double-layer metallic subwavelength slit arrays," *Opt. Lett.* **31**, 516–518 (2006).
11. C. Cheng, J. Chen, Q. Wu, F. Ren, J. Xu, Y. Fan, and H. Wang, "Controllable electromagnetic transmission based on dual-metallic grating structures composed of subwavelength slits," *Appl. Phys. Lett.* **91**, 111111 (2007).
12. R. M. Bakker, V. P. Drachev, H. K. Yuan, and V. M. Shalaev, "Enhanced transmission in near-field imaging of layered plasmonic structures," *Opt. Express* **12**, 3701–3706 (2004).
13. Z. Marcet, J. W. Paster, D. W. Carr, J. E. Bower, R. A. Cirelli, F. Klemens, W. M. Mansfield, J. F. Miner, C. S. Pai, and H. B. Chan (2008) "Controlling the phase delay of light transmitted through double-layer metallic subwavelength slit arrays," *Opt. Lett.* **33**, 1410–1412 (2008).
14. S. Astilean, P. Lalanne, and M. Palamaru "Light transmission through metallic channels much smaller than the wavelength," *Opt. Commun.* **175**, 265–273 (2000).
15. Y. Takakura, "Optical resonance in a narrow slit in a thick metallic screen," *Phys. Rev. Lett.* **86**, 5601–5603 (2001).
16. F. Yang and J. R. Sambles, "Resonant transmission of microwaves through a narrow metallic slit," *Phys. Rev. Lett.* **89**, 063901 (2002).
17. C. H. Gan and G. Gbur, "Strategies for employing surface plasmons in a near field transmission optical readout system," *Appl. Phys. Lett.* **91**, 131109 (2007).
18. C. H. Gan and G. Gbur, "Strategies for employing surface plasmons in near-field optical readout systems," *Opt. Exp.* **14**, 2385–2397 (2006).
19. G. Gbur, H. F. Schouten and T. D. Visser, "Achieving superresolution in near-field optical data readout systems using surface plasmons," *Appl. Phys. Lett.* **87**, 191109 (2005).
20. A. Degiron and T. W. Ebbesen, "Analysis of the transmission process through single apertures surrounded by periodic corrugations," *Opt. Express* **12**, 3694–3700 (2004).
21. H.J. Lezec, A. Degiron, E. Devaux, R. A. Linke, L. Martín-Moreno, F. J. García-Vidal, and T. W. Ebbesen, "Beaming light from a subwavelength aperture," *Science* **297**, 820–822 (2001).
22. M. Scalora, M. J. Bloemer, A. S. Pethel, J. P. Dowling, C. M. Bowden, and A. S. Manka, "Transparent, metallo-dielectric, one-dimensional, photonic band-gap structures," *J. Appl. Phys.* **72**, 2377–2383 (1998).
23. M. J. Bloemer and M. Scalora, "Transmissive properties of Ag/MgF₂ photonic band gaps," *Appl. Phys. Lett.* **83**, 1676–1678 (1998).
24. S. Feng, J. M. Elson, and P. L. Overfelt, "Optical properties of multilayer metal-dielectric nanofilms with all-evanescent modes," *Opt. Express* **13**, 4113–4124 (2005).
25. F. García-Vidal, H. J. Lezec, T. W. Ebbesen, and L. Martín-Moreno, "Multiple paths to enhance optical transmission through a single subwavelength slit," *Phys. Rev. Lett.* **90**, 213901 (2003).
26. W. L. Barnes, A. Dereux, and T. W. Ebbesen, "Surface plasmon subwavelength optics," *Nature* **424**, 824–830 (2003).
27. J. W. Goodman (2005) *Introduction to Fourier Optics*, Roberts & Company, Englewood, 3rd edition.
28. P. B. Johnson, and R. W. Christy, "Optical constants of the noble metals," *Phys. Rev. B* **6**, 4370–4379 (1972).
29. L. Martín-Moreno, F. J. García-Vidal, H. J. Lezec, K. M. Pellerin, T. Thio, J. B. Pendry, and T. W. Ebbesen, "Theory of extraordinary optical transmission through subwavelength hole arrays," *Phys. Rev. Lett.* **86**, 1114–1117 (2001).
30. N. Bonod, S. Enoch, L. Li, E. Popov, M. Nevière, "Resonant optical transmission through thin metallic films with and without holes," *Opt. Express* **11**, 482–490 (2003).
31. S. A. Darmanyan and A. V. Zayats, "Light tunneling via resonant surface plasmon polariton states and the enhanced transmission of periodically nanostructured metal films: An analytical study," *Phys. Rev. B* **67**, 035424 (2003).
32. A. Giannattasio, I. R. Hooper, and W. L. Barnes, "Transmission of light through thin silver films via surface plasmon polaritons," *Opt. Express* **12**, 5881–5886 (2004).
33. T. D. Visser, H. Blok, and D. Lenstra, "Theory of polarization-dependent amplification in a slab waveguide with anisotropic gain and losses," *IEEE J. Quantum Electron.* **35**, 240–249 (1999).
34. E. Palik (1985) *Handbook of Optical Constants of Solids*, Academic Press, New York.
35. N. N. Rao (2004) *Elements of Engineering Electromagnetics*, Prentice Hall, New Jersey, 6th edition.
36. D. K. Cheng (1994) *Fundamentals of Engineering Electromagnetics*, Addison-Wesley, Massachusetts.

1. Introduction

Extraordinary optical transmission (EOT) through corrugated thin metal films and subwavelength-aperture arrays in metal plates has evoked great interest since its first experimental demonstration by Ebbesen *et al.* [1]. Although there are still continuing discussions on the physical mechanism in play, the critical role of surface plasmons in EOT has been confirmed

through several studies [2, 3, 4, 5, 6, 7].

More recently, EOT with plasmonic arrays arranged in cascade have been investigated [8, 9, 10, 11]. It was found that the optical transmission through the cascaded layers either exceeded or was comparable to the transmission through a single layer. While these recent investigations focused primarily on two layers in cascade, here we will consider up to five cascaded layers. Proposed applications of such cascaded structures include the improvement of surface enhanced Raman scattering, light confinement and guidance at the nanoscale, SNOM capabilities, and control of the phase delay of the transmitted light [12, 13].

Through rigorous numerical simulations, we show that corrugated metallic films arranged in cascade can potentially impede the exponential decay of electromagnetic fields that is otherwise characteristic of optically thick metal slabs. The impeding of the field decay often leads to optical transmission greater than that due to Fabry-Perot resonance-like behavior [14, 15, 16] exhibited by subwavelength slits in a single slab, in which the transmission oscillates through maxima and minima as a function of the plate thickness. Hereafter, we refer to this impedance or suppression of the field decay as a phenomenon of EOT. In this sense, EOT is achieved when more light is transmitted through an optical system than expected due to the effects of absorption.

We seek to demonstrate that an appreciable fraction of the optical power that is incident on a multi-layered system can be transmitted over distances greater than the skin depth of the metal. The geometry of the layered structures considered in the present study is motivated by previous investigations on achieving plasmon-assisted super-resolution in near field optical readout systems [18, 17]. It was found there that the performance of the readout system could be improved or degraded with suitably placed ‘plasmon pits’ on a metal film, taken to be silver in that case. Besides enhancement of the coupling between surface plasmons and light, these plasmon pits serve to increase the transmission and/or confine the electromagnetic fields between them, depending on whether they are present on the illuminated or dark side of the metal film [19, 21, 20]. Research by others on metallo-dielectric, one-dimensional photonic crystal structures, albeit different from the structures investigated in the present study, have also revealed a high degree of transparency over thickness of hundreds of skin depths [22, 23, 24].

In Section 2 of this paper, the geometries of the proposed multi-layered structures and their single slab equivalent are presented. Specifically, the multi-layered system is made up of thin metallic films which either have (a) a pair of plasmon pits on both surfaces, or (b) a pair of plasmon pits only on the illuminated side of the film. To perform rigorous simulations of the electromagnetic fields in these structures, we have adopted a Green tensor method that will be briefly described in Section 3. Results for the two multi-layered structures are presented separately in Sections 4 and 5. In section 6, the field enhancement effects of the two structures are compared by defining an “effective skin depth” δ for each of the structures. This is followed by section 7, where we further discuss the important role of the surface plasmons for the enhanced field effects observed in the simulated multi-layered structures before finally offering concluding remarks.

2. Proposed multi-layered structures

We consider placing two pairs of plasmon pits ‘back to back’ on the surfaces of a thin metal film. Each of these films, of thickness t , can be cascaded to form a multi-layered structure with an air gap g separating them, as shown in Fig. 1a. The pair of plasmon pits on each surface are laterally separated by a distance of 2γ . As it has been suggested that the grooves on the dark side only contribute weakly to the plasmon-assisted enhanced transmission [20, 25, 26], we will also investigate structures with plasmon pits only on the illuminated side of the metal plates, as shown in Fig. 1b. These structures are more favorable for experiment than those

in Fig. 1a because they could be fashioned through an alternating process of deposition and etching, making them more suitable for nano-fabrication. The geometry shown in Fig. 1c is that of a single slab with equivalent thickness and volume as a n -layered system ($n = 1, 2, 3, \dots$) for either one of the multi-layered structures in Fig. 1.

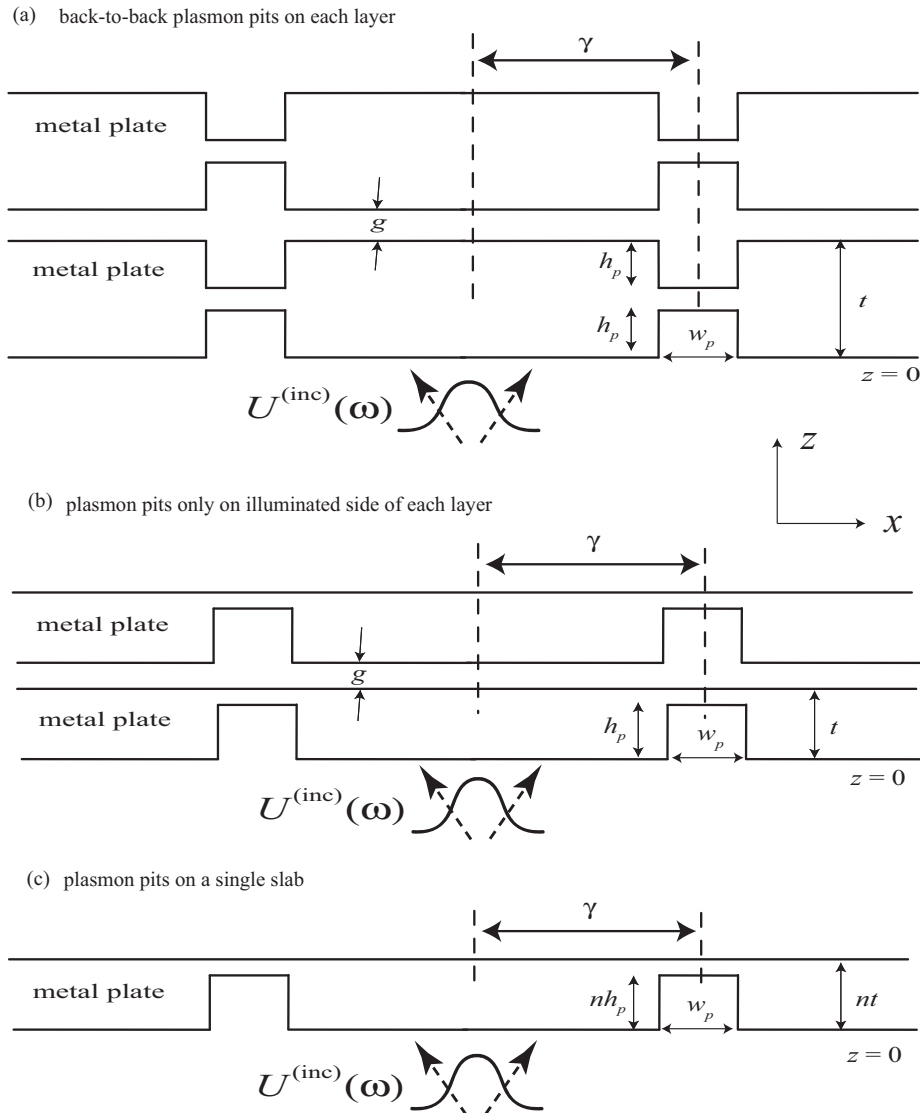


Fig. 1. Geometry for the multi-layered structure with two layers for (a) plasmon pits on both sides of the metal films, and (b) plasmon pits only on the illuminated side of the metal films. More layers of identical metal films may be cascaded. The geometry shown in (c) is that of a single slab with equivalent thickness and volume as a n -layered system ($n = 1, 2, 3, \dots$) of either structure (a) or (b).

For the ensuing discussion, it is taken that the structures in Fig. 1 are illuminated at normal incidence with quasi-monochromatic light at a wavelength (λ) of 500 nm, around the middle of the visible spectrum. The incident light is taken to be a Gaussian beam with beamwidth at full width at half maximum of 530 nm, and is synthesized in the simulations with an angular

spectrum of plane waves [27]. We take the metal films to be silver, which typically exhibits low absorption losses in the visible region of the spectrum. The refractive index of silver at $\lambda = 500$ nm is taken to be $n_{ag} = 0.05 - i2.87$, following the data of Johnson and Christy [28].

The optical transmission T , i.e. the optical power emerging from the structures, is normalized to the incident field such that

$$T = \frac{\int_{-\infty}^{+\infty} S_z dx}{Y_0 \int_{-\infty}^{+\infty} |E^{(inc)}(x, z)|^2 dx}, \quad (1)$$

where S_z is the normal component of the time-averaged Poynting vector emerging from the data layer, $Y_0 = \sqrt{\frac{\epsilon_0}{\mu_0}}$, and $E^{(inc)}(x, z)$ is the electric field amplitude of the incident Gaussian beam.

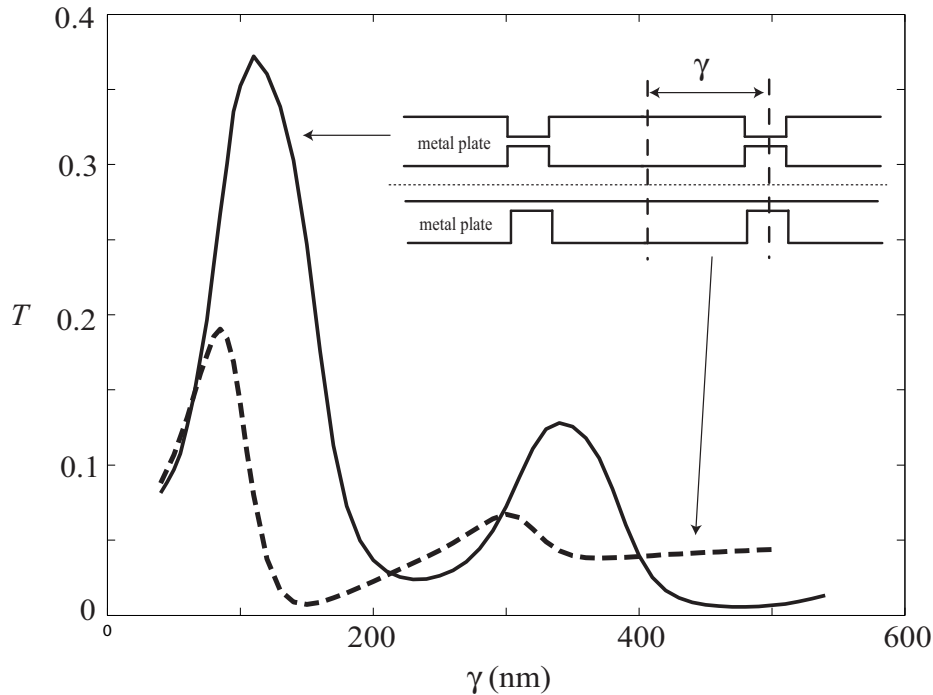


Fig. 2. Optical transmission T as a function of γ for a single layer of the structures depicted in Fig. 1a (solid line) and Fig. 1b (dashed line).

The gap g is kept small in this case so that surface plasmons propagating on surfaces separated by the air gaps can couple resonantly with each other [8, 29]. We take g to be 20 nm and 10 nm for the multi-layer structure in Fig. 1a and Fig. 1b, respectively. The thickness t of the silver plate is taken to be 100 nm and 50 nm for the structure in Fig. 1a and Fig. 1b, respectively. The thickness of the silver plates are chosen to be thin both to decrease absorption losses and to enhance resonant plasmon coupling [30]. The height h_p and width w_p of each plasmon pit in the multi-layered structures are both taken to be 40 nm in this case.

It is to be noted that both the separation g and the thickness t for the multi-layered structure in Fig. 1b have been taken to be half of that in Fig. 1a. Such a choice would allow us to compare the transmission between structures that have an equal volume of metal but has different number of layers for the geometries in Fig. 1(a) and (b). The value of γ is taken to be 80 nm, as simulations with a single layer ($n = 1$) of the multi-layered structures in Fig. 1 show optimal optical transmission for values of γ between 70 and 90 nm for both cases (see Fig. 2).

Since the quantity of interest is the optical transmission T , it is reasonable to pose the question: why not simply have slits in the metal plates instead of the plasmon pits? It would seem that when compared to the slit, the plasmon pit differs only in an additional thin barrier layer which attenuates propagating fields. However, it has been demonstrated by several groups that enhanced transmission of light through metallic thin films without perforating apertures can be attributed to resonant light tunneling via surface plasmons on the surfaces of the films [31, 30, 32]. As we will see in section 7, the optical transmission through the multi-layered structures in Fig. 1 can indeed be greater than that for multi-layered slit structures of equivalent thickness in some cases.

3. The Green tensor method

To simulate the electromagnetic interactions between light and surface plasmons in the proposed structures, we have adopted a two-dimensional planar layered geometry for which the Green tensor can be calculated analytically up to within a Fourier transform. In this method, the electric field can be determined through the numerical solution of a domain integral equation [33] of the form,

$$E_i(x, z) = E_i^{(inc)}(x, z) - i\omega \int_D \Delta\epsilon(x', z') G_{ij}^E(x, z; x', z') E_j(x', z') dx' dz' \quad (2)$$

where E_i represents the i th component ($i = x, y, z$) of the total electric field, $E_i^{(inc)}$ represents the incident field which would propagate in the system in the absence of the plasmon pits, ω is the angular frequency of the field, and G_{ij}^E is the Green tensor of the ideal layered medium. The integral is over all regions D (the plasmon pits) in which the system deviates from the ideal layered geometry. $\Delta\epsilon$ is the difference in permittivity between the 'deviant' regions and the background system.

This equation can be solved numerically within the deviant regions by the collocation method with piecewise-constant basis functions. The field everywhere else may then be calculated by substitution back into Eq. (2). The incident field can be either TE-polarized (\mathbf{E} perpendicular to the $x-z$ plane) or TM-polarized (\mathbf{H} perpendicular to the $x-z$ plane). However, due to the invariance of the system along the y -axis, only incident TM-polarized light will excite surface plasmons.

Let us denote the total thickness of the structures shown in Fig. 1 as

$$z_T = \begin{cases} nt + (n-1)g & \text{for multi-layered systems in Fig. 1(a) and (b);} \\ nt & \text{for equivalent single slab in Fig. 1(c),} \end{cases} \quad (3)$$

with n being the number of layers for the multi-layered structures. In calculating the optical transmission T as defined in Eq. (1), the normal component of the time-averaged Poynting vector S_z is determined through the relation

$$\langle \mathbf{S} \rangle = \frac{1}{2} \text{Re}[\mathbf{E} \times \mathbf{H}^*], \quad (4)$$

evaluated at $z = z_T$. Here the angular brackets and the asterisk denote time-averaging and complex conjugation, respectively.

For the structures considered in this study, the fields \mathbf{E} and \mathbf{H} in Eq. (4) are calculated via the Green tensor method we have described. In a practical implementation, the optical transmission T could be measured with suitably placed detectors collecting the light emerging from the system of thin films at various angles. As we are interested in enhanced field effects associated with surface plasmons, it will be taken that the structures in the following simulations are illuminated with TM-polarized light, unless otherwise specified.

4. Numerical simulations for pits on both surfaces of metal

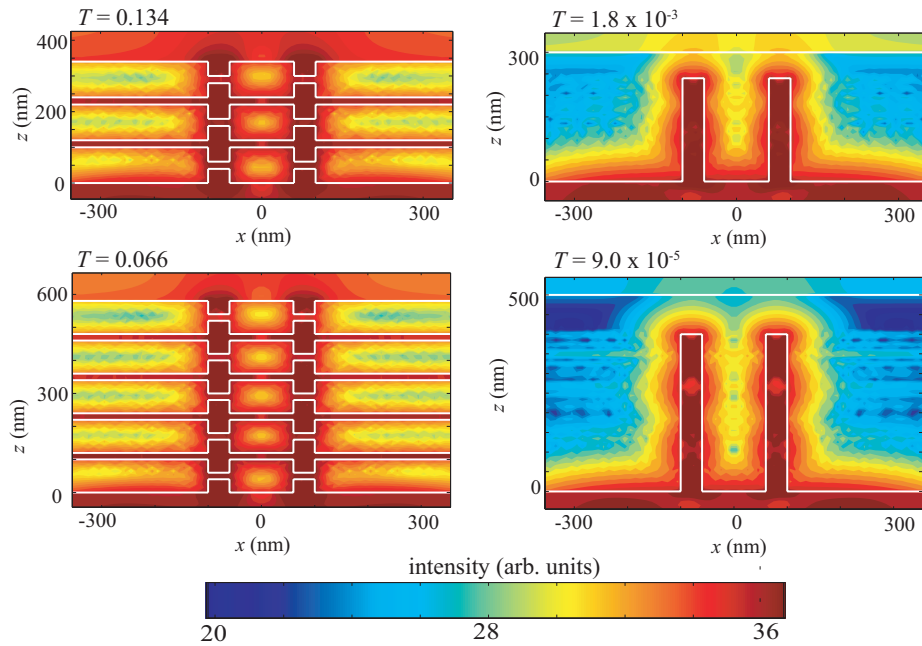


Fig. 3. Field distribution plots depicting the impedance to exponential decay of the fields with the multi-layered structure in Fig. 1a as opposed to a single metal slab with equivalent thickness and volume for number of layers $n = 3$ and 5. EOT for the multi-layered structures is clearly observable from the values of the associated optical transmission T .

To demonstrate the ability of the multi-layered structure of Fig. 1a to impede the exponential decay of the field, we compare its optical transmission T and field intensity distribution with those of the single slab. Typical results for the field intensity distributions are shown in Fig. 3, where $\gamma = 80$ nm. The optical transmission T for $n = 1$ to 5 are shown in Table 1.

It is clear from the results of Fig. 3 and Table 1 that while the field in the single slab decays very quickly as it penetrates through the material (skin depth for silver at $\lambda = 500$ nm is ~ 15 nm), the field decay in the multi-layered structure is relatively insignificant, even in the layer furthest from the incident field. This is true even when the number of layers is increased progressively from $n = 1$ to $n = 5$. In these cases ($n = 1$ to 5), the transmission T through the multi-layered structure is much greater than that through the single silver slab with equivalent volume of metal. Even when $n = 1$, it can be seen that the transmission is improved significantly just by having four plasmon pits instead of two. This demonstrates that EOT is achievable with the proposed multi-layered structure.

To show that these effects are due to surface plasmons, and not waveguide modes or other possible evanescent modes, we repeated the simulations for tungsten films illuminated by TM-polarized light, and for silver films illuminated with TE-polarized light. The refractive index of tungsten at $\lambda = 500$ nm is taken to be $n_w = 3.38 - i2.68$, following the data of Palik [34].

As the absorption (imaginary part of n_w) in tungsten is very close to that of silver ($n_{ag} = 0.05 - i2.87$), one might expect similar behavior in the optical transmission. It is to be noted however, that tungsten does not support surface plasmons at this frequency, since $\epsilon'_w > 0$, ($\epsilon_w = n_w^2 = \epsilon'_w - i\epsilon''_w$). In the case of TE-polarized light, no surface plasmons are excited because the

Table 1. Optical transmission T for multi-layered structures (up to $n = 5$ layers) of Fig. 1a, as compared to a single metal slab with equivalent thickness. The transmission T is evaluated at z_T (nm), where z_T is the total thickness of the structure. The superscripts § and † denote the multi-layered structure and the single slab, respectively. For compact presentation, e^{-m} is used as short form for $\times 10^{-m}$.

| n | 1 | 2 | 3 | 4 | 5 |
|-----------------|-------|-------|-------------|-------------|-------------|
| z_T^{\S} | 100 | 220 | 340 | 460 | 580 |
| T^{\S} | 0.233 | 0.185 | 0.134 | 0.096 | 0.066 |
| z_T^{\dagger} | 100 | 200 | 300 | 400 | 500 |
| T^{\dagger} | 0.035 | 0.012 | $1.8e^{-3}$ | $6.3e^{-4}$ | $9.0e^{-5}$ |

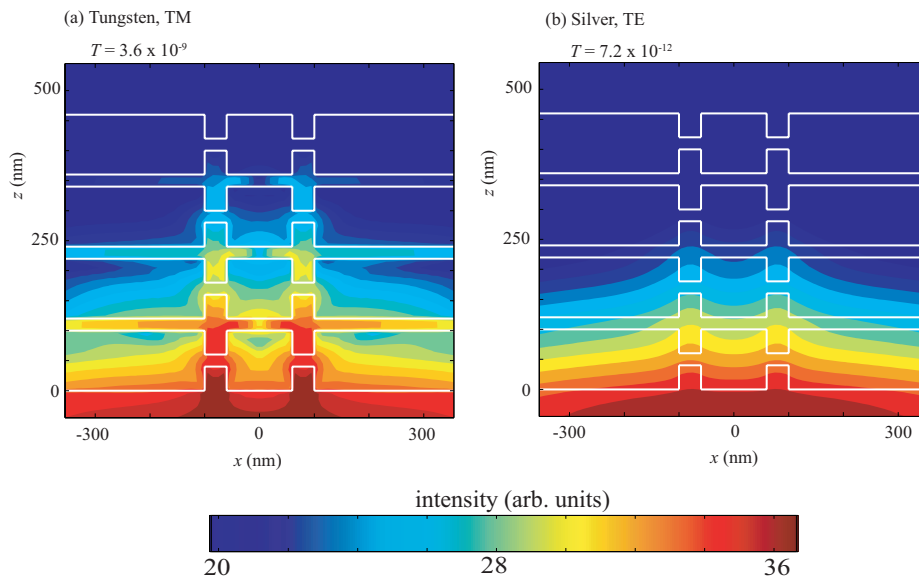


Fig. 4. Field distribution plots for (a) tungsten multi-layered structure with TM-polarized light, and (b) silver multi-layered structure with TE-polarized light, for number of layers $n = 4$.

boundary conditions cannot be matched for surface plasmons at the interfaces. As such, both these structures do not support surface plasmons.

For a subwavelength slit of width a , the cutoff wavelength for the TE dominant waveguide mode is $\lambda_c = 2a$ [35, Sec 8.2]. Since our plasmon pits are only 40 nm wide, waveguide modes are not supported as well for the TE case. For a slit in the TM case, the TM_0 mode is a special case of the TEM (transverse electromagnetic) mode, having no cutoff [36, Sec 9.2]. Therefore one can expect very low optical transmission for the TE case. Typical results are shown in Fig. 4,

where it has been taken that the number of layers $n = 4$. Clearly, no enhanced field effects can be observed from the the field distribution plots for these two structures, unlike what we have seen in Fig. 3. Furthermore, the optical transmission T is extremely low, orders of magnitude lower than for the case where surface plasmons are supported.

Table 2. Optical transmission T for misaligned multi-layered structures of Fig. 1a for $n = 3$, compared to an aligned structure with $\gamma = 80$ nm (see Fig. 3). The transmission T is evaluated at $z_T = 340$ nm. The superscripts \S , $(m, 1)$, and $(m, 2)$ denote the perfectly aligned case and two cases that are slightly misaligned.

| n | 1 | 2 | 3 | T |
|------------------|----|----|----|-------|
| γ^{\S} | 80 | 80 | 80 | 0.134 |
| $\gamma^{(m,1)}$ | 90 | 78 | 84 | 0.128 |
| $\gamma^{(m,2)}$ | 86 | 81 | 77 | 0.116 |

Since the alignment of these multi-structured layers can be a daunting task in actual experiments, we have investigated how sensitive these effects are when there is some misalignment between each layer. Typical results are presented in Table 2. It is seen that the effects on the field decay are not dramatically different, and the transmission does not vary significantly (less than 15% reduction) from the perfectly aligned case ($T = 0.134$). Therefore, slight misalignments in the multi-layered structure do not cause drastic changes to the response of the multi-layered system.

5. Numerical simulations for pits only on illuminated side of metal films

Though the multi-layered structures proposed in Fig. 1a can significantly impede exponential decay of fields in a single metallic slab, it is conceivable that these structures present challenges for precise nano-fabrication. In this respect, the multi-layered structures with plasmon pits only on the illuminated side of the metal films as depicted in Fig. 1b might be more palatable for practical implementation. The results for the optical transmission T for $n = 1$ to 5 are shown in Table 3, where γ is again taken to be 80 nm.

As seen from Table 3, similar impeding of the field decay can still occur, although the effects are less prominent, and the EOT less significant. Also, for the cases $n = 4$ and 5, the transmission through the pits in the single film is greater than that for the multi-layered structure. These are instances where the impeded decay of the field with the multi-layered structure do not give rise to transmission greater than the single slab. This is not necessarily surprising as the transmission through each of the pits is subject to a Fabry-Perot resonance behavior.

To demonstrate the Fabry-Perot nature of the plasmon pits, it is useful to consider a long, narrow pit as a slit that is covered with a thin barrier. It is reasonable then to expect that the effect of light propagating through the additional thin metal barrier roughly corresponds to a shift both in the magnitude and phase of the transmitted field. We have performed simulations for a single slit and pit of slit width 40 nm ($\lambda = 500$ nm), and the results are shown in Fig. 5. As expected, the optical transmission through the long, narrow pit exhibits a Fabry-Perot resonance type behavior, similar to the case of the subwavelength slit.

Table 3. Optical transmission T for multi-layered structures (up to $n = 5$ layers) of Fig. 1b, as compared to a single metal slab with equivalent thickness. The superscripts \ddagger and \dagger denote the multi-layered structure and the single slab, respectively. For compact presentation, e^{-m} is used as short form for $\times 10^{-m}$.

| n | 1 | 2 | 3 | 4 | 5 |
|------------------|-------|-------|-------|-------------|-------------|
| z_T^{\ddagger} | 50 | 110 | 170 | 230 | 290 |
| T^{\ddagger} | 0.185 | 0.089 | 0.029 | $8.0e^{-3}$ | $2.0e^{-3}$ |
| z_T^{\dagger} | 50 | 100 | 150 | 200 | 250 |
| T^{\dagger} | 0.185 | 0.035 | 0.012 | 0.012 | 0.021 |

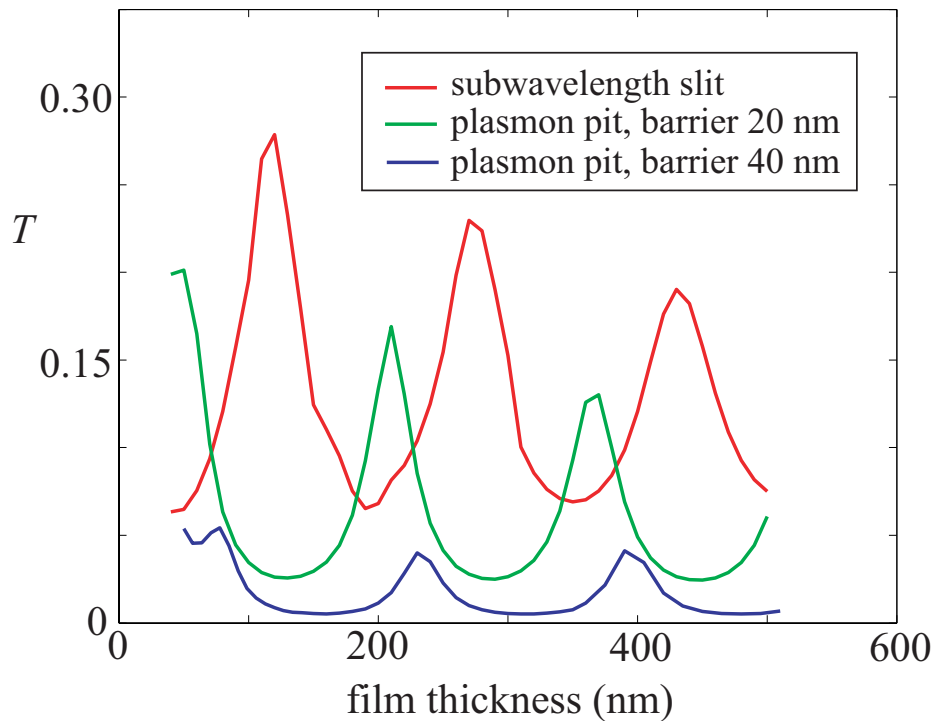


Fig. 5. Illustrating the shift in the magnitude and phase of the Fabry-Perot resonance transmission when subwavelength slits in a metal plate is replaced by narrow pits, such as those shown in Fig. 1c. The red, green, and blue lines represent transmission for a pair of slits, pits with 20 nm barrier, and pits with 40 nm barrier, respectively. In all cases, the slits or pits are separated by $2\gamma = 160$ nm.

6. Comparison of the two multi-layered systems - effective skin depth

We are now in a position to ask which of the two multi-layered structures in Fig. 1 is more effective in producing field enhancement effects in the system. As noted before, the structure

in Fig. 1a can be much more challenging in terms of nano-fabrication. What is the advantage it provides over the structure in Fig. 1b, if there is any? Is it possible to quantify the field enhancement in the multi-layered structures as compared to the single slab? To deal with these questions, we have plotted in Fig. 6 the transmission T for the different structures. Our observations led us to define an “effective skin depth” δ for the structures, as we explain below.

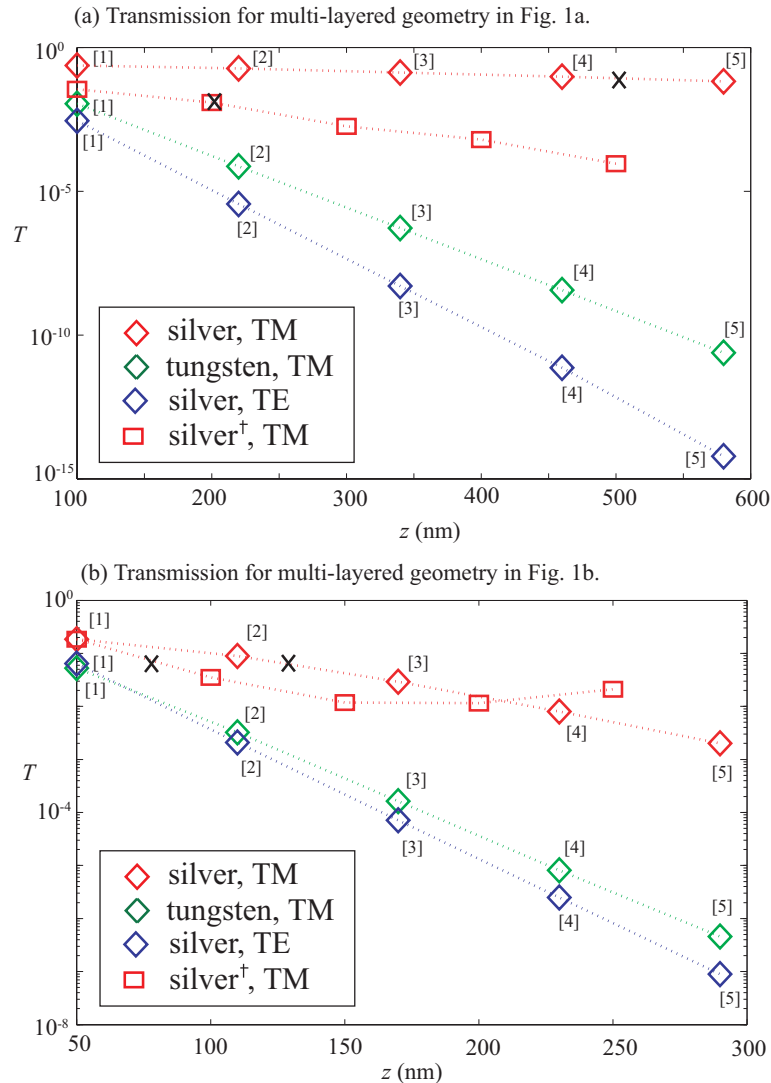


Fig. 6. Comparison of the transmission T as a function of z , for (a) the multi-layered geometry in Fig. 1a, and (b) the multi-layered geometry in Fig. 1b. The superscript \dagger is used to refer to the equivalent single slab structure. Data for the multi-layered and equivalent single slab structures are indicated with empty diamonds and boxes respectively. The number in [] indicates the number of layers in the multi-layered structure. The ‘x’ indicates the extrapolated value of the “effective skin depth” δ . It is to be noted that δ is defined as the thickness at which the transmitted intensity has dropped to 36.79 % of the value for which $n = 1$.

Compared to the single slab, it is seen that the multi-layered structure is often superior in

terms of the optical transmission. Also, the enhanced field effects are more prominent for the case where plasmon pits are positioned back-to-back on each of the films, i.e., the system of Fig. 1a. As the thickness of the single slab increases, the effects of the skin depth predominate over the Fabry-Perot like behavior of the pits to suppress the optical transmission. In addition, the structures that support surface plasmons are capable of optical transmission much higher than the structures that do not. These results, which support our claim that surface plasmons are responsible for the observed EOT, have been observed in Figs. 3 - 5. The importance of the role of the surface plasmons in producing the enhanced field effects will be further discussed in the next section.

A closer look at the curves in Fig. 6 reveals that the transmission exhibits a linear logarithmic relationship with the number of layers (n), or equivalently, the overall thickness of the structures (z_T). This logarithmic relationship is observed for all the structures investigated except the case of the equivalent single slab of the multi-layered geometry of Fig. 1b illuminated by TM-polarized light. As explained above, this is due to the Fabry-Perot resonance in the narrow plasmon pit when the thickness of the barrier is thin enough so that absorption effects do not predominate.

In view of the logarithmic dependence of the transmission for most cases, it seems reasonable to define an effective skin depth (δ) for the structures, where δ is the thickness at which the transmitted intensity has dropped to 36.79 % of the value for which $n = 1$. As appreciable optical transmission is associated with structures where surface plasmons are present, we have extrapolated the effective skin depth δ from the transmission curves only for these cases, i.e., the silver structures with TM illumination. For the equivalent single slab of the multi-layered geometry of Fig. 1b, only the first three data points ($n = 1$ to 3) are used for the extrapolation.

For the geometry of Fig. 1a, we find that $\delta \sim 400$ nm and 100 nm for the multi-layered system and equivalent single slab, respectively. For the geometry of Fig. 1b, we find that $\delta \sim 75$ nm and 25 nm for the multi-layered system and equivalent single slab, respectively. For both cases, we find that the skin depth for the multi-layered system can be 3 or 4 times more than the equivalent single slab. The multi-layered structure therefore has the effect of extending the skin depth significantly for propagating optical fields that are incident on the system. For the multi-layered structures with plasmon pits only on the illuminated side (Fig. 1b), this is true at least for $n \leq 3$. For $n \gg 5$, it is expected that, with a corresponding increase in the thickness of the metal barrier above the plasmon pit, absorption effects would dominate the transmission as in the case of the equivalent single slab of the structure of Fig. 1a.

7. Further discussion and conclusion

To strengthen our claim that surface plasmons are responsible for these enhanced field effects, we performed another series of simulations with more plasmon pits on each of the layers, keeping the same incident Gaussian beam as before. Each of the plasmon pits can serve to enhance the light-plasmon coupling, and to confine the fields through the reflection of the plasmons at the edges. By having three plasmon pits instead of two on each side of the metal films, we expect the surface plasmon effects to be enhanced.

Results for the simulated optical transmission T for the three-pit structures are compared with their corresponding two-pit structures in Table 4. It is seen that for the three-pit case, there is a significant increase in the achievable EOT, giving approximately 2.4 and 1.9 times higher transmission than the two-pit multi-layered structures of Fig. 1a and Fig. 1b, respectively. The suppression of the field decay, or equivalently the effective skin depth δ is also increased to approximately 480 nm and 125 nm, respectively. These results provide evidence that the enhanced coupling between light and surface plasmons is critical to achieving the enhanced field effects in the multi-layered structures.

Table 4. Comparison of the optical transmission T with three plasmon pits instead of two in each of the silver layers for the multi-layered structures of Fig. 1a, and Fig. 1b. The superscripts § and ‡, denote the multi-layered structure of Fig. 1a, and the multi-layered structure of Fig. 1b, respectively. An additional numeric superscript 3 is used to denote structures with three plasmon pits on each silver layer.

| n | 1 | 2 | 3 | 4 | δ (nm) |
|------------------|-------|-------|-------|-------------|---------------|
| z_T^{\S} | 100 | 220 | 340 | 460 | – |
| $T^{\S,3}$ | 0.579 | 0.422 | 0.309 | 0.227 | 480 |
| T^{\S} | 0.233 | 0.185 | 0.134 | 0.096 | 400 |
| z_T^{\ddagger} | 50 | 110 | 170 | 230 | – |
| $T^{\ddagger,3}$ | 0.344 | 0.173 | 0.056 | 0.016 | 125 |
| T^{\ddagger} | 0.185 | 0.089 | 0.029 | $8.0e^{-3}$ | 75 |

Next, we consider if the same effects can be achieved with perforated slits instead of plasmon pits, since the former is perceivably a simpler structure to implement in practice. As mentioned before, enhanced optical transmission through metallic thin films with only surface corrugations can be attributed to resonant light tunneling via surface plasmons on the surfaces of the films. Repeating the simulations with slits in place of the plasmon pits, we find that similar field impeding effects can also be observed for the slits' structure. The results for the optical transmission T are shown in Table 5.

By comparing with results in the above tables, it can be seen that the optical transmission T with the plasmon pits is greater in some cases. In fact, for the case of the multi-layered system of Fig. 1a, T is always greater with the pits than with the slits in our simulations. Therefore, it can be advantageous to employ the plasmon pits instead of the slits in the multi-layered structures in practical applications.

To conclude, we have demonstrated numerically the occurrence of extraordinary optical transmission (EOT) in multi-layered systems of metallic thin films. Comparing the optical transmission of a Gaussian beam that is normally incident on the multi-layered system with that transmitted from a single slab with equivalent thickness and volume of the metal, it was found that the usual decay of the field intensity in the single slab can be significantly suppressed in the layered system. These enhanced field effects can occur over multiple layers of metal films (up to five in our simulations) arranged in cascade. Total absence of these enhanced field effects in simulations with TE (transverse electric) polarized light and in materials that do not excite surface plasmons supports our claim that these effects are plasmon-mediated. Furthermore, the enhanced field effects are more profound when more pits are added on each of the surfaces to increase the coupling between light and surface plasmons.

To quantify these field enhancement effects, we have introduced an effective skin depth δ for the multi-layered systems, which we found can be many times greater than the skin depth of a metal slab. In our study, the skin depth of silver is ~ 15 nm at $\lambda = 500$ nm. The striking

Table 5. Simulations of the optical transmission T with slits in place of the plasmon pits of the multi-layered structures in Fig. 1. The superscripts § and ‡, denote the multi-layered structure of Fig. 1a, and the multi-layered structure of Fig. 1b, respectively. The additional superscript ‘slit’ is used to denote the structures with slits. These values should be compared with their counterparts of Table 1 ($T^{\text{§}}$) and Table 3 ($T^{\text{‡}}$).

| n | 1 | 2 | 3 | 4 | 5 |
|----------------------|-------|-------|-------|-------|-------|
| $z_T^{\text{§}}$ | 100 | 220 | 340 | 460 | 580 |
| $T^{\text{§, slit}}$ | 0.196 | 0.102 | 0.047 | 0.022 | 0.011 |
| $z_T^{\text{‡}}$ | 50 | 110 | 170 | 230 | 290 |
| $T^{\text{‡, slit}}$ | 0.064 | 0.071 | 0.076 | 0.062 | 0.040 |

suppression of the field decay over distances much longer than the skin depth in these multi-layered structures offers potential for application in near field optical systems where enhanced field effects are desired. It is hoped that with advances and improvements to the processes for nano-fabrication of such multi-layered structures, cascaded corrugated metal films will find a host of interesting applications in future nano-optical technologies.

Acknowledgements

This research was supported by the Department of Energy under Grant No. DE-FG02-06ER46329.